A NUMERICAL STUDY OF REINFORCED EMBANKMENT-SUPPORTED BY ENCASED FLOATING COLUMNS

NUMERIČNA ŠTUDIJA OJAČENIH NASIPOV, PODPRTIH Z OBLOŽENIMI GRUŠČNATIMI STEBRI

Mehmet Rifat Kahyaoğlu *(corresponding author)*
Muğla Sitki Kocman University, Engineering Faculty,
Department of Civil Engineering
48000, Mentese-Muğla, Turkey
E-mail: rkahyaoglu@mu.edu.tr

Martin Vaníček
Geosyntetika Ltd.
N.Tesla str. 3, 160 00 Praha 6, The Czech Republic
E-mail: mvanicek@geosyntetika.cz

DOI https://doi.org/10.18690/actageotechslov.16.2.25-38.2019

Keywords

geogrid reinforcement, geotextile encasement, surcharge, soil settlement, column bulging, sand mat

Ključne besede

geomreže, geotekstilna obloga, preobremenitev, posedanje zemljine, izbočenje stebra, peščena podlaga

Abstract

This paper presents a three-dimensional, finite-element, parametric study of a base-reinforced embankment supported by encased floating columns on soft soil. A 3D numerical model is made to study the effects of geogrid basal reinforcement and geotextile encasement on the displacement behavior of the columns. The numerical model was initially verified using measured data from a real case study. Then, parametric studies were subsequently performed, considering the effect of the encasement stiffness, the basal reinforcement stiffness and the embankment fill height, together with an examination of the effective length of the encasement. The results from this parametric study are presented here in the form of comparative graphs. The objective of this paper is to present the behavior of the embankment on floating encased columns after the soft soil consolidation for different embankment heights, basal reinforcement and column-encasement stiffnesses.

Izvleček

V prispevku je predstavljena tridimenzionalna parametrična študija končnih elementov ojačenega nasipa, podprtega z geotekstilom obloženimi gruščnatimi stebri na mehkih tleh. Izdelan je 3D numerični model za proučevanje učinkov osnovne ojačitve z geomrežo in geotekstilnih oblog na deformacijsko obnašanje gruščnatih stebrov. Numerični model smo sprva preverili s pomočjo študije izmerjenih podatkov na realnem primeru. Nato so bile naknadno izvedene parametrične študije ob upoštevanju učinka togosti geotekstilnih oblog, togosti osnovne ojačitve z geomrežo in višine polnilnega nasipa vzdolž raziskovane efektivne dolžine geotekstilnih oblog. Rezultati iz te parametrične študije so predstavljeni v obliki primerjalnih grafov. Cilj tega prispevka je predstaviti obnašanje nasipa ležečega na z geotekstilom obloženih gruščnatih stebrih po konsolidaciji mehkih tal za različne višine nasipov, osnovne ojačitve in togosti z geotekstilom obloženih stebrov.

1 INTRODUCTION

The construction of embankments on soft soils, as part of the efforts to reclaim new areas for the construction of highways, railways, airport runways and urban infrastructure, faces several hurdles with regard to the low load-bearing capacity and high compressibility of the subsoil, as well as the tendency for excessive lateral deformations. Among the various available techniques, such as surcharging, excavation and replacement, vertical drainage, vacuum consolidation and column-

-supported embankments, the use of column-supported embankments (CSEs) allows for a rapid construction, total and differential settlement reduction, and adjacent facility protection [1-3]. However, it is impossible to construct CSEs in very soft clays (cu < 15 kN/m2) due to the insufficient columns material lateral confinement and excessive lateral bulging of the columns [4-6].

In such soils, the required lateral confinement can be induced through the encasement of individual columns with geosynthetics [7-11]. In 1995 the first project utilizing a seamless geotextile-encased column was successfully implemented in Germany, and later, Kempfert et al. [5], Raithel and Kempfert [6] and Raithel et al. [7] tested the performance of geosynthetic-encased stone columns (GECs) using numerical and analytical models. The technique detailed in the above-mentioned projects has been adopted in Europe [8, 9] and more recently in South America [11], but with growth in the construction sector and improvements in geosynthetic production technologies, new design procedures have been developed.

The performance of geosynthetic encasement on the capacity and settlement behavior of soft soils has been studied in both laboratory and field tests [12-17], while numerical studies of encased granular columns have been conducted successfully in the literature [18-27]. The cited studies investigated the influence of the geometry and material properties of encased and non-encased stone columns (SCs) on vertical stresses, excess pore-water pressures and tangential strains in the geotextile, with a focus on the effect of encasement length and stiffness, the strength of the soft ground and surcharge from the embankment fill. The benefit of encasing stone columns in terms of settlement, lateral deformation and load-carrying capacity has been underlined in the above studies, and design charts for an estimation of the maximum settlement in soil and column strain during the preliminary design are presented.

In recent years, in the event of high embankment loads, one layer of geogrid has been used at the base of the embankment in combination with GECs over soft clay soils to form a geosynthetic reinforced and column-supported embankment (GRCSE) [28-30]. The application of a geogrid layer over the columns and the soft soil enhances the efficiency of the load transfer from the embankment to the columns, provides controllable deformation, minimizes soil yield, enhances global stability and eliminates the need for inclined columns to resist the horizontal thrust at the sides of the embankment [31-34]. The complicated mechanism of load transfer in GRCSEs combines with the arching effects, tension in the geosynthetic reinforcement and stress transfer from the soft soil to the column due to the different stiffness values. Over the past few years, both experimental and numerical investigations into the behavior of GRCSE have been carried out by many researchers [35, 37]. Previous studies have analyzed the performance of GECs and the time-dependent behaviors of geosynthetic-reinforced embankments supported on end-bearing columns.

In some instances, when the column does not reach a hard stratum, the construction of floating columns is found to be more economical and technically feasible. The frictional force along the floating column, based on the relative deformation between the column and the surrounding soil, affects the behavior of GECs [36, 38, 39]. Although previous research has contributed valuable information to the knowledge of end-bearing columns, information about the group behavior of floating columns is still lacking, and so further research is required into the design of embankments on encased floating columns [40-42].

This paper explores the time-dependent behavior of geogrid-reinforced embankments supported by floating columns encased in geotextiles. Firstly, a real case study of GRCSE in thick soft soil was modeled numerically. Then, the numerical results and the measured data were compared, and some calibrations on the numerical model were made for the verification. Finally, parametric studies including variations of the embankment height, the stiffness of the column encasement and the base reinforcement were performed.

Many of the recent studies mentioned above have dealt with the load-carrying capacities and settlement of unreinforced embankments supported with GECs; however, the effects of reinforcement to the base of the embankment have not been considered to date, nor have the load-transfer mechanism and the lateral bulging deformation patterns associated with GECs. The published literature focusing on the long-term effects of these parameters on the vertical and lateral displacement behaviors of the GECs is limited, and so in order to enhance the performance of the GECs to contribute to the above-mentioned issues, the objectives of this paper are as follows: (1) to examine the long-term behavior (100% consolidation) of a floating, column-supported embankment under different surcharges; (2) to investigate the performance of basal geogrid reinforcement; (3) to consider the effects of geotextile encasement on the lateral and vertical displacement of columns; and (4) to determine the effective length of the geotextile encasement of floating columns.

2 NUMERICAL MODELLING

2.1 Model verification

A case study of a stone-column-supported embankment constructed in Kebun-Malaysia, the details of which can be found in Raju (1997) [43], was modelled numerically. The soil profile for the Kebun Interchange project contained marine clay where the CPT tip resistance values for the top 11 m are 0.1–0.3 MPa (Fig 1). Stone columns with a 1.1-m diameter were installed at a 2.2-m rectangular spacing to a depth of 12 m under the 2.6-m-high embankment. Settlement gauges were placed on the top of the stone columns and the total settlement was read as 0.4 m. A 1-m settlement was observed for untreated ground under the same circumstances. The results of the settlement in the soft soil and the encased column after the completion of the embankment construction from our numerical model were compared with measured settlements from the Kebun project. This comparison presented in Fig. 2 shows that the numerical model followed the trends of the measured data. The vertical stress transmitted to both the stone column and the soft soil was verified with measured values, and this consistency indicates that the numerical model is appropriate for a parametric study.

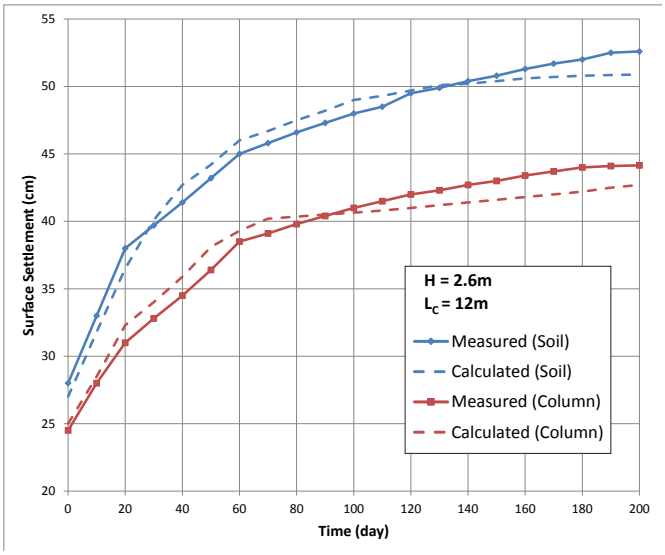

Figure 2. Comparison between the calculated and measured settlements of the column and the soil.

2.2 Parametric study

GRCSE in 40-m-thick soft soil lying on a rigid and firm layer were modeled and studied numerically. The water level was modelled at the original ground surface. Floating columns having a diameter of 1 m (D) were arran-

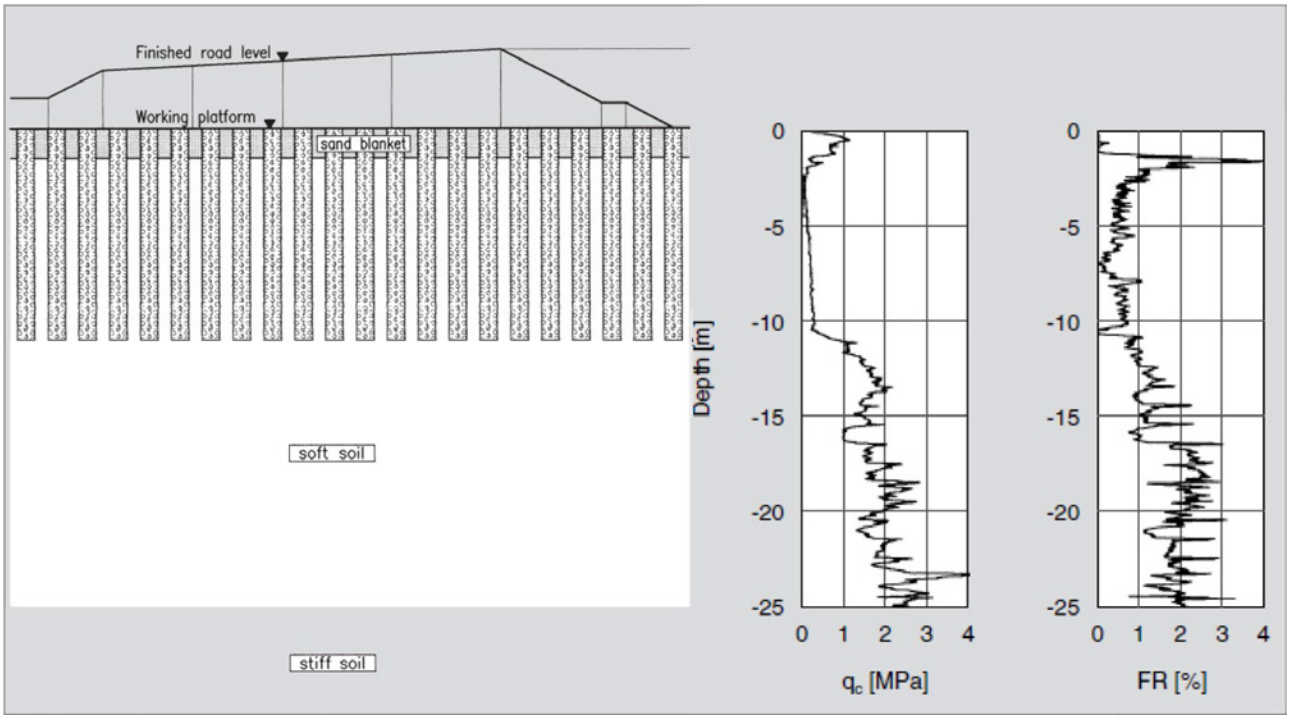

Figure 1. Schematic section view of Kebun Case (Raju, 1997) and tip resistance (q_c) - friction ratio (FR) with depth.

ged in a square-grid pattern with a 3-m center-to-center spacing, giving an area replacement ratio of 8.7 percent. All the stone columns were encased with geotextiles of the best geosynthetic type for the encasement of the floating columns [20]. A 1-m-thick sand mat, acting as a working platform below the embankment (2V:1H side slopes), was established on top of the natural clay soil prior to the embankment fill to allow equipment access and to provide drainage for the columns. Furthermore, one layer of geogrid was laid to provide a basal reinforcement for the embankment.

The numerical analyses were carried out using an available PLAXIS 3D Foundation package [44]. The displacements and the vertical stresses on the column and the surrounding soil, as well as the tensile strains and tangential tensile forces acting on the geosynthetics, were calculated. The details of the cross-section of the model and the finite-element mesh are shown in Fig. 3, representing the right half of the domain on account of the symmetry.

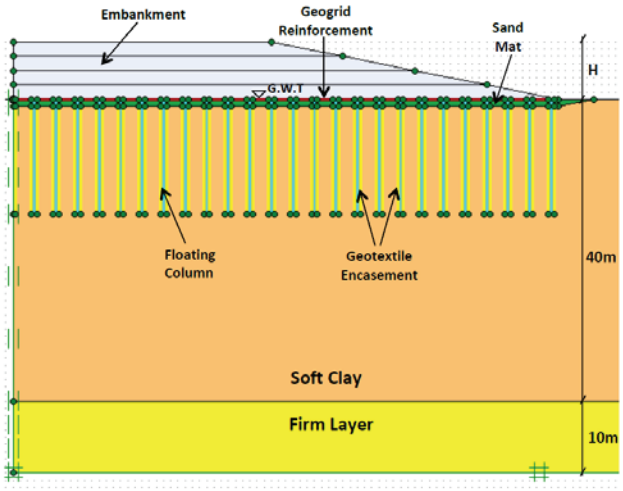

Figure 3a. Cross-section of the model.

In the analyses, the model limits were 50 m in the vertical direction and 220 m in the horizontal direction, being five times the width of half of the embankment base, so as to minimize the boundary effect. Fig. 4 shows the finite-element mesh used in the 3D numerical simulations. The soil clusters were modeled using 10-noded tetrahedral elements, whereas the geosynthetic elements are represented by 6-noded triangle surface elements. A horizontal displacement was not permitted on the vertical boundaries of the model; however, the bottom boundary was fixed securely in both the vertical and horizontal directions.

The embankment fill construction to the top surface was simulated in four stages. For each stage 20 days was envisaged for the construction of a 2-m layer and 90 days for the consolidation from its surcharge. The consolidation analyses were carried out during and after each construction stage. After the completion of the embankment construction, the calculations were continued until the excess pore-water pressure dissipation at mid-depth of the clay layer had reached 1 kPa. A closed consolidation boundary was applied to the sides of the model parallel to the embankment axis to prevent lateral drainage.

Both the embankment fill and the sand mat (assumed to be Sacramento River sand) were modeled using the Mohr–Coulomb failure criterion under a drained condition. Kaliakin et al. [45] discussed the determination of the values from experimental data for Sacramento River sand based on the tests carried out by Lee and Seed [46]. The column material was modeled as granular soil, in

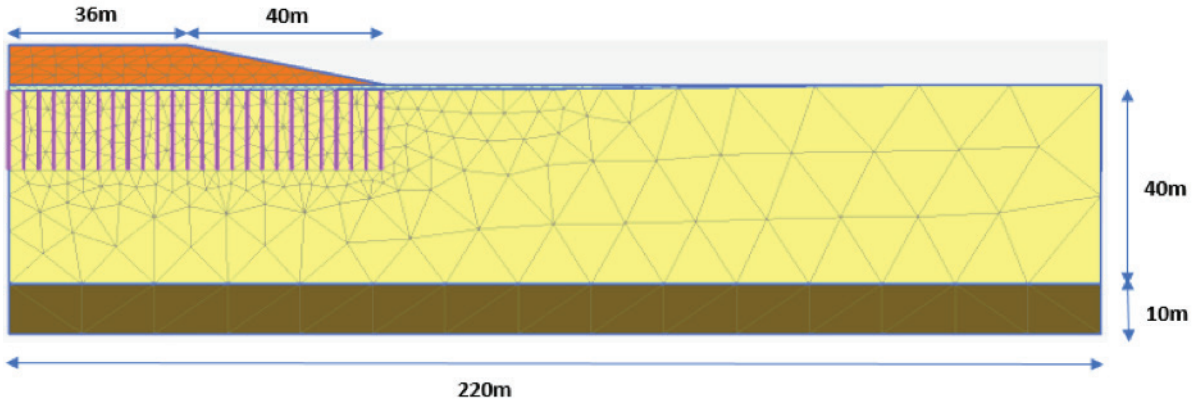

Figure 3b. Cross-section of the finite-element model.

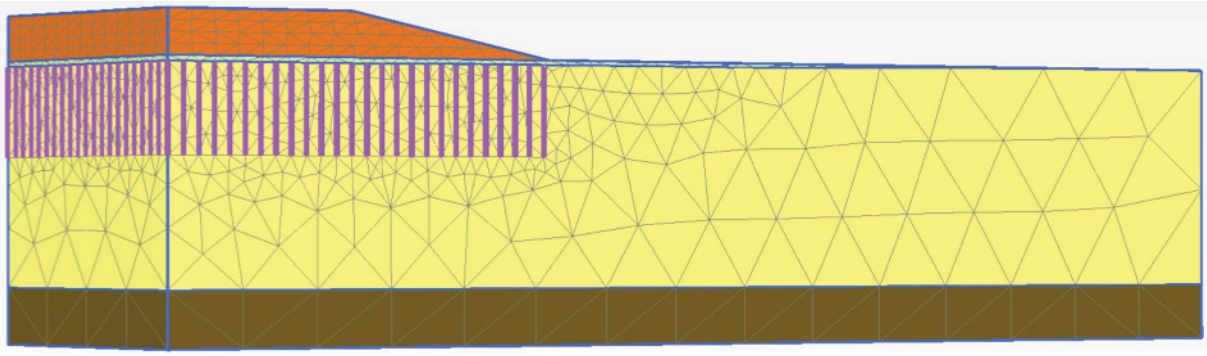

Figure 4. 3D finite-element model.

line with the suggestions of Ambily and Gandhi [47]. The soft soil was idealized using the modified Cam Clay (MCC) model. The MCC parameters considered in this study were adopted from the geotechnical parameters of soft Kebun clay soil encountered in a recent soft-ground improvement project [43]. Khabbazian et al. [37] stated that the use of the MCC model is preferable over the Mohr–Coulomb or linear elastic models, in that it allows a more accurate modeling of the behavior of the soft soil.

The geosynthetics used for both the reinforcement and the encasement were modeled as linear elastic material with no bending stiffness, as recommended by Murugesan and Rajagopal [19] and Liu et al. 2007 [13]. The stiffness of the geosynthetic reinforcement (J=EA) was determined as the tensile force at 3% elongation divided by that elongation (3%). Perfect adhesion between the stone and the surrounding soil were assumed, and thus interface elements with a rigid interface were used at the interfaces of either the stone column and the encasement, or the encasement and the soft clay [22, 23]. In fact, a large number of researchers have been investigating so much to characterize the interface working mechanism and propose fruitful achievements on the constitute models of the soil-geosynthetic interface. The parameters used in the numerical analyses are summarized in Table 1.

Stone columns are installed using vibro-displacement and vibro-replacement methods. The stone material is laterally expanded, which is accompanied by an increase in the horizontal earth pressure and the excess pore-water pressure in the soft soil during and after the column's installation. However, any influence related to the installation of the columns was disregarded in this study.

Table 1. Material parameters used in the numerical analyses.

Parameter	Column Material *Stone Soil* (Ambily and Gandhi 2007)	Embankment Fill *Sacramento River Sand* (Kaliakin 2012)	Working Platform *Sacramento River Sand* (Kaliakin 2012)	Soft Clay *Kebun Clay* (Raju 1997)
Model Type	Mohr-Coulomb	Mohr-Coulomb	Mohr-Coulomb	Modified Cam Clay
Unit Weight, γ(kN/m^3)	24	22.5	20	15
Effective Friction Angle, ϕ'(°)	42	36	32	-
Effective Cohesion, c'(kPa)	1	1	1	-
Dilation Angle, φ'(°)	10	4	3	-
Elastic Modulus, E(kPa)	55000	20000	15000	-
Poisson's Ratio, ν	0.3	0.3	0.3	0.3
Slope of Swelling Line, K	-	-	-	0.02
Slope of the Virgin Consolidation Line, λ	-	-	-	0.4
Void Ratio at Unit Pressure, e	-	-	-	1.0
Slope of the Critical State Line, M	-	-	-	1.0
Permeability, k(m/s)	1×10^{-2}	1×10^{-3}	1×10^{-3}	1×10^{-6}

In order to cover all the cases in the embankment--construction scenarios, parameters such as the embankment height (H), column-encasement stiffness (J_E), and basal reinforcement stiffness (J_R) were varied, as summarized in Table 2.

Table 2. Parameters evaluated in the parametric analyses.

Parameter					
Embankment Height, H (m)	2	4	6	8	
Geogrid Reinforcement Stiffness, J_R (kN/m)	1000	2000	3500	5000	6500
Column Length, L_C (m)	16				
Geotextile Encasement Stiffness, J_E (kN/m)	500	1000	1500	2000	2500

For the case of the 8-m-high embankment, the critical length of a floating column according to the analytical equation developed by Satibi [40] was determined as 15 m. Based on this critical length, the lengths of the columns are determined to be 16 m (L_C=16m) for the whole parametric study. A comparison is made of the surface settlement of the column and the soft soil, the column bulging, the vertical stresses on the floating column (L_C=16m) and the soft soil, and the tangential force in the geogrid reinforcement.

A similar parametric study with several variables for reinforced shallow foundations was performed by Jelušič and Žlender [48, 49].

3. RESULTS OF THE PARAMETRIC STUDY

The results of the parametric study evaluating the variation of the embankment height, column encasement and basal reinforcement stiffnesses were categorized according to the effects on the stress strain behavior of the GRCSE in the following subsections.

3.1 Surface settlement

Fig. 5 shows the surface-settlement behavior of the encased columns and the soft soil for different unreinforced embankment cases. The results reveal a significant decrease in the settlement with the encasement, which is thought to be a direct consequence of the column bulging reduction by additional confining pressure produced by the geotextile encasement along the column length. It is also clear that an increase in the stiffness of the encasement improves the performance of the GEC.

The settlement curves (Fig. 5) also indicate that geotextile encasement reduces the total settlement, but generates some differential settlement. The soft soil closer to the embankment centerline is subjected to greater vertical stresses when compared to the soil near the embankment edges, leading the settlement values to decrease with the distance from the centerline of the embankment. The value of the maximum settlement of the column close to the middle is about 30 percent greater than that of the column near the edge. The settlement response of the GECs also depends strongly on the surcharge from the embankment's self-weight. When the embankment height is less than 4.0 m (H < 4 m), the surface settlements are small.

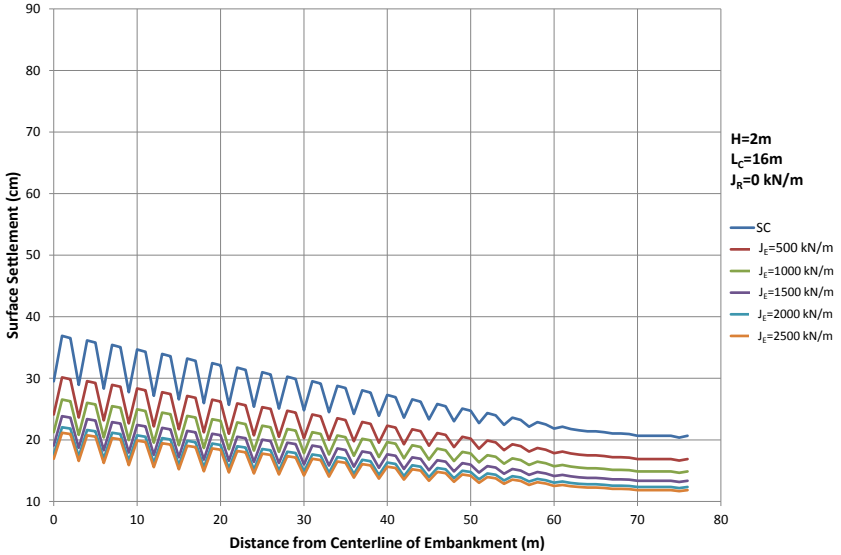

Figure 5a. Settlement profile at the base of the embankment; H=2m.

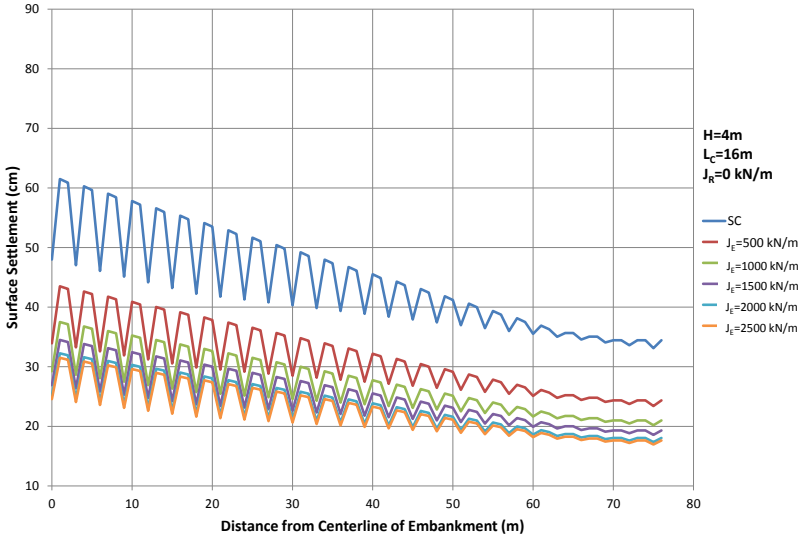

Figure 5b. Settlement profile at the base of the embankment; H=4m.

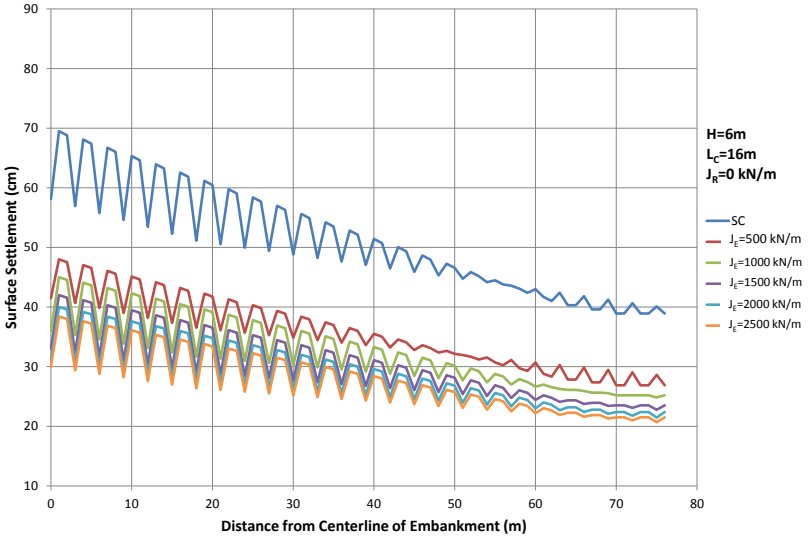

Figure 5c. Settlement profile at the base of the embankment; H=6m.

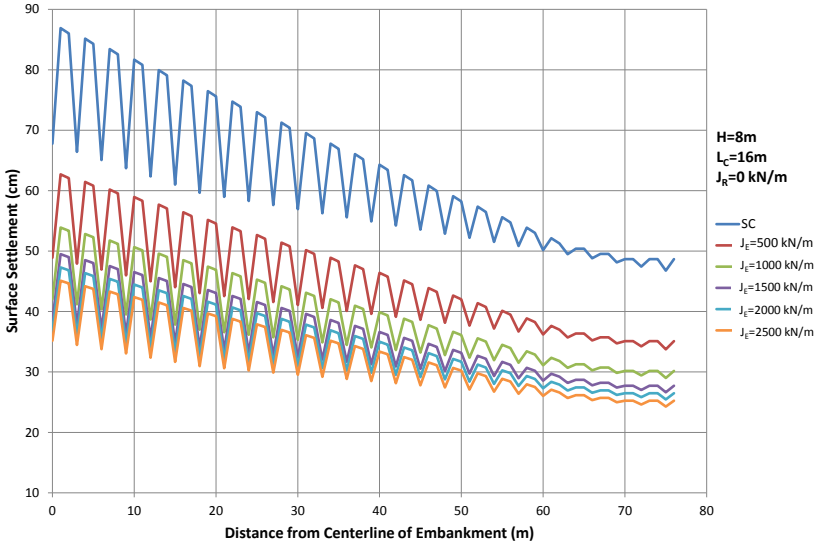

Figure 5d. Settlement profile at the base of the embankment; H=8m.

The settlement-reduction factor (β = ratio of the settlement for stabilized soft clay over the settlement of untreated soft clay) is almost equal to 0.82 (H=2 m) when the encased column (J_E=500 kN/m) is used. For H=2 m, the average settlement value on the soil decreases by 17 percent, and on the column by 18 percent. As the stiffness value of the encasement increases, β decreases to 0.49. For small stiffness values of the encasement ($J_E \leq$ 1500kN/m), β decreases gradually, while for higher stiffness values, it remains approximately constant (Fig. 6).

Fig. 7 illustrates the surface-settlement behavior of the encased columns (J_E=500kN/m) and the soft soil in the case of the reinforced embankment base. For H=2 m, the settlement value of the soil in the center of the embankment decreased from 15.8 cm to 10.4 cm, and of the column from 11.8 cm to 7.8 cm. The results show that the surface-settlement values of the soft soil and the column with the base reinforcement reduced by 35 and 34 percent, respectively. Keeping the stiffness value of the encasement constant, if the reinforcement stiffness increases, the settlement value decreases, as would be expected. For low stiffness values of the basal reinforcement, the settlement value decreases much more significantly, while for higher values, the settlement change becomes less noticeable and remains approximately

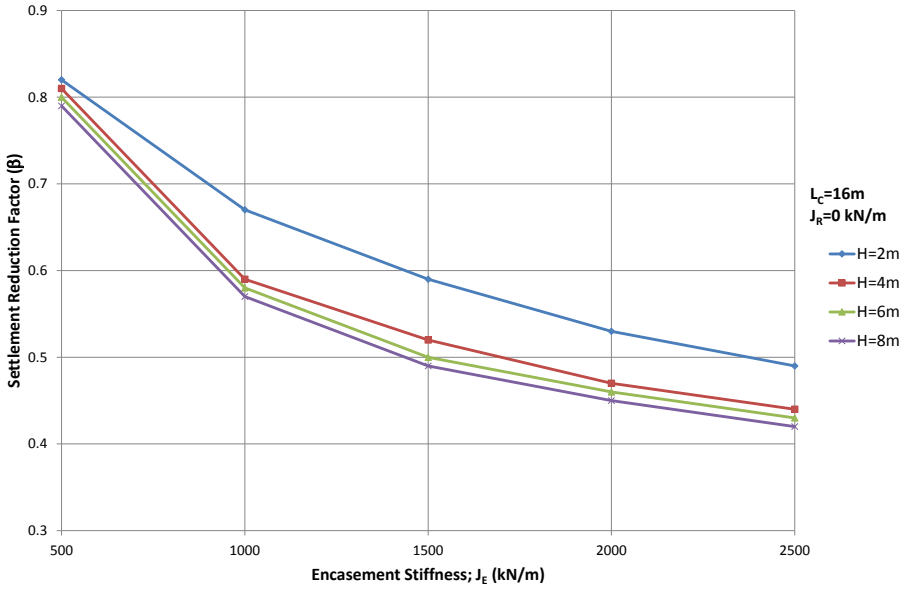

Figure 6. Variation of the settlement reduction ratio with the encasement stiffness.

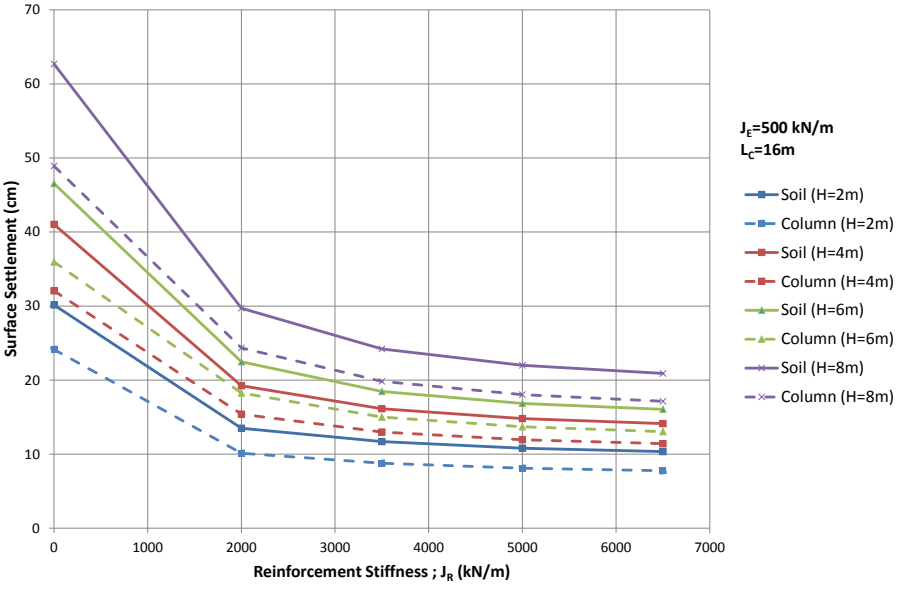

Figure 7. Variation of the settlement with the load intensity relative to the reinforcement stiffness.

constant. This means that although the geogrid has a positive effect on reducing the settlement of the soft soil beneath the embankment, this effect does not increase as the stiffness of the geogrid increases.

3.2 Lateral displacement of the columns

An encased column offers greater resistance to bulging as a result of the mobilized tangential stresses in the geotextile; consequently, higher stresses are transferred to greater depths, resulting in a decrease in the bulging [24-26]. The lateral displacements of the SC and GEC with different encasement-stiffness values under different surcharges are shown in Fig. 8. The column is displaced laterally within the soft soil as a result of loading, especially in the upper part. For H=2m, the SC exhibits considerable lateral bulging (12.4 mm), whereas the maximum lateral bulging of the GEC is limited (1.5 mm). However, after a depth of 1D, the GEC experienced more lateral displacement than the SC. This is attributed to the column confinement and the stress redistribution within the GEC [30].

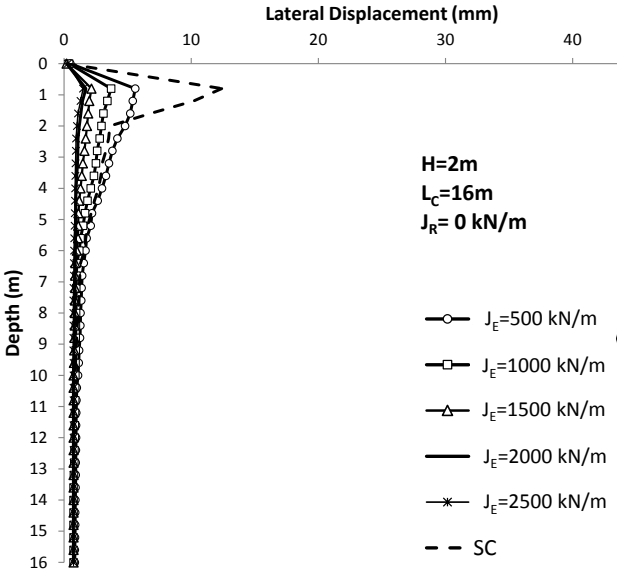

Figure 8a. Lateral displacement distribution of the columns at the end of the consolidation; H=2m.

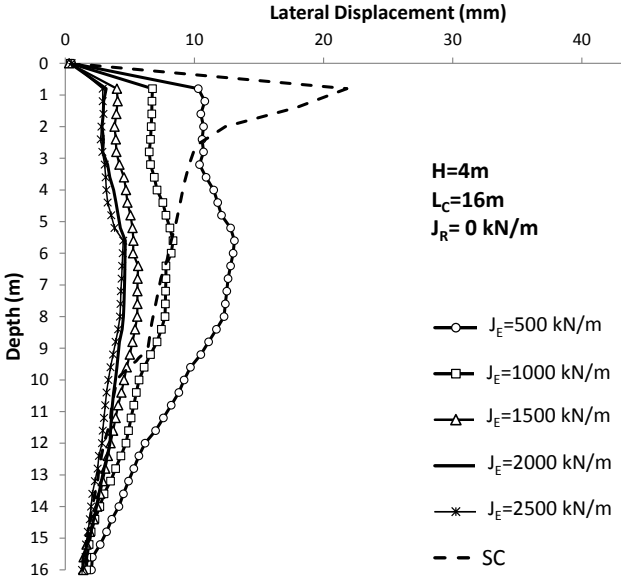

Figure 8b. Lateral displacement distribution of the columns at the end of the consolidation; H=4m.

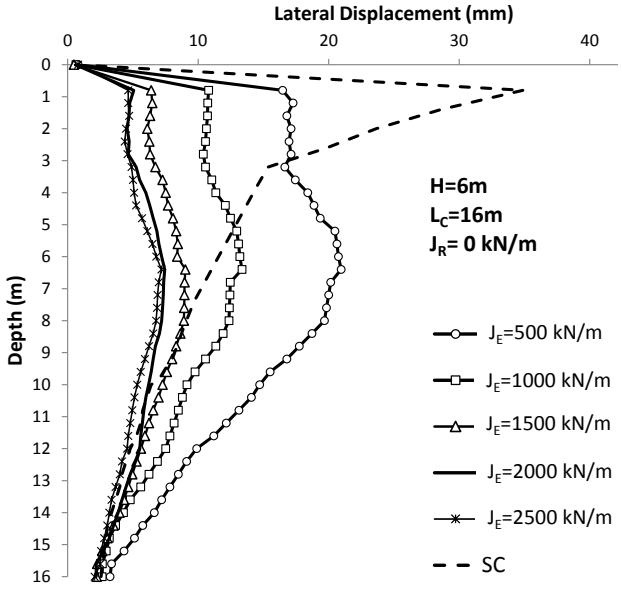

Figure 8c. Lateral displacement distribution of the columns at the end of the consolidation; H=6m.

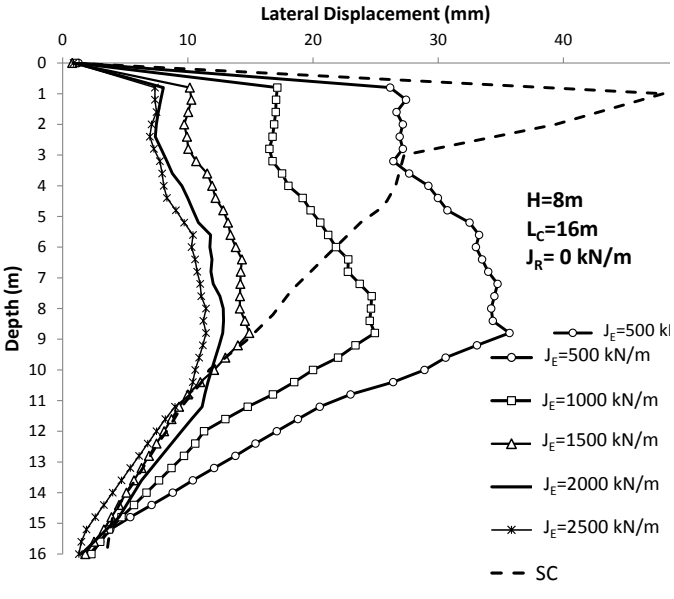

Figure 8d. Lateral displacement distribution of the columns at the end of the consolidation; H=8m.

Fig. 8 also shows that increasing the encasement stiffness up to 1500 kN/m results in a decrease in the lateral displacement; however, for higher stiffness values, the change in the lateral displacement is insignificant. It is clear that the bulging along the column increases with increasing load, causing more stress transfer to the lower depths during consolidation. For a relatively low embankment height, the bulging occurs mainly in the upper 1.5D zone. As the embankment height increases, the bulging zone extends downwards, with the maximum lateral displacement occurring at 8D below the top of the column. This finding is noteworthy, in that other researchers have previously attempted to find a specific value for the optimum length of the geosynthetic [24, 25]. This trend shows that an efficient design for an optimum encasement depth is related to the surcharge from the embankment, the column and the soft soil properties, and so full encasement could be necessary to ensure a bulging reduction.

3.3 Vertical stress below the embankment

After the completion of the construction, vertical stresses on the soft soil decrease with consolidation as a result of the redistribution of the forces. In contrast, vertical stresses on the encased columns continue to an increase during consolidation. This load transfer from the soil to the column can be quantified using a stress-concentration ratio (SCR), defined as the ratio of an average vertical stress on top of a column to the average vertical stress on the top of soft soil. The SCR plays a substantial role in reducing the stress in the soil, which leads to the settlement reduction. As the degree of load transfer between the column and the soil depends largely on the stiffness ratio between the column and the subsoil, the SCR can be expected to be larger for a GEC than for a SC. Experimental studies made on non-encased columns [21] demonstrate that the SCR on the whole varies between 2 and 3, but can reach 20 in some cases of geosynthetic-encased granular columns. Typical reported values of the SCR for piled embankments (without geogrid reinforcement) range from 1 to 8 [50, 51]; however, the calculated SCR in this study varies between 1.2 and 3.2, which contradicts previous studies [22, 23, 25]. This value can be explained by means of using the sand-working platform instead of applying the embankment load directly onto the soft soil. The presence of the sand working platform, the higher the embankment transfer from the embankment to the surrounding soil, a result of which is that the SCR remains lower than expected. The relationship between the SCR and the reinforcement stiffness is presented in Fig. 9.

As can be seen from Fig. 9, the vertical stresses on both the encased column and the surrounding soil increase as the embankment height increases, and the rate of the increase is higher for a reinforced case, pointing to the fact that basal reinforcement is highly effective in promoting the arching. The effect of reinforcement (referring to reinforcement stiffness) becomes more remarkable when the surcharge is greater. British Standard BS8006-1:2010 "Code of practice for strengthened/reinforced soil and other fills" implements the design for a geosynthetic reinforced-pile-supported embankment to evaluate the stress-reduction ratio, which represents

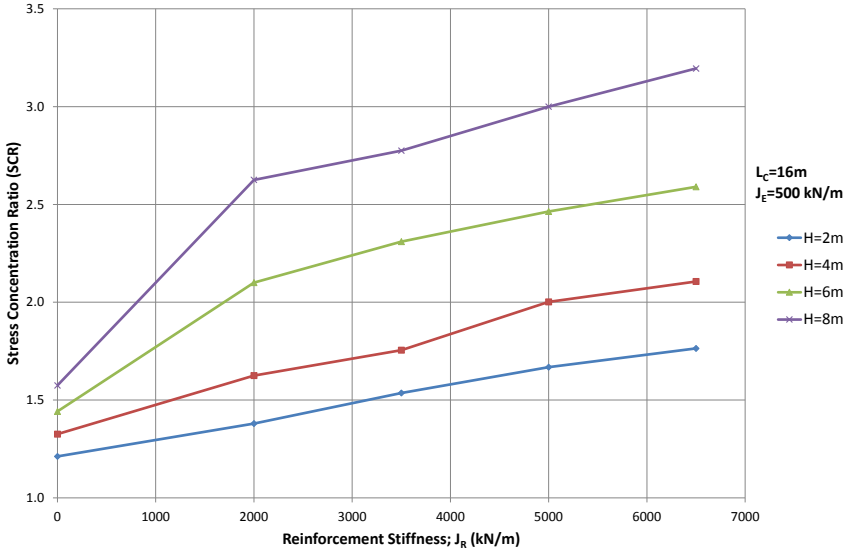

Figure 9. Variation of the stress-concentration ratio load intensity relative to the reinforcement stiffness.

the portion of the load from the embankment on to geosynthetics and between the piles. The computation considers factors such as the column (pile) diameter, the column spacing, the embankment fill height, the unit weight of fill used, the friction angle of the embankment and the stiffness of the geosynthetic.

3.4 Tension force in the basal reinforcement

When the soft soil settles in between the columns, the geogrid reinforcement layer elongates, resulting in a tension force that reduces the net pressure on the soft soil. The vertical stress above the geogrid layer is greater than that below the geogrid, and this effect helps the transfer the loads to the columns. The calculated tension forces along the geogrid layer decrease as the distance from the centerline of the embankment increases (Fig. 10).

The maximum computed acting force is only around 20% of the design strength of the geogrid, and this small force is consistent with the relatively small computed differential settlement between the column and the soil. The maximum tension force in the geogrid increases with its tensile stiffness (Fig. 11). The largest strain of the geogrid is 3%, which is in accordance with the suggested strain values [52, 53].

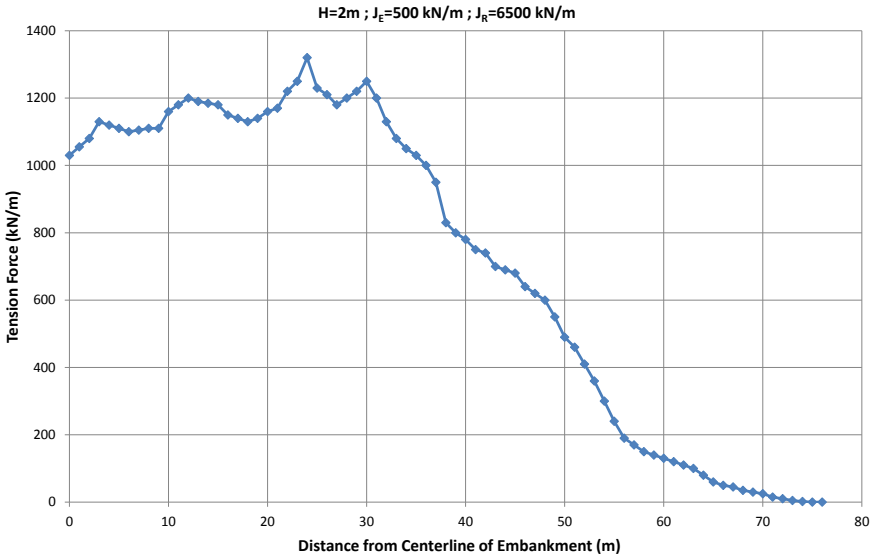

Figure 10. Distribution of the tension force along the geogrid layer (H=2m, J_E=500kN/m, J_R=6500kN/m).

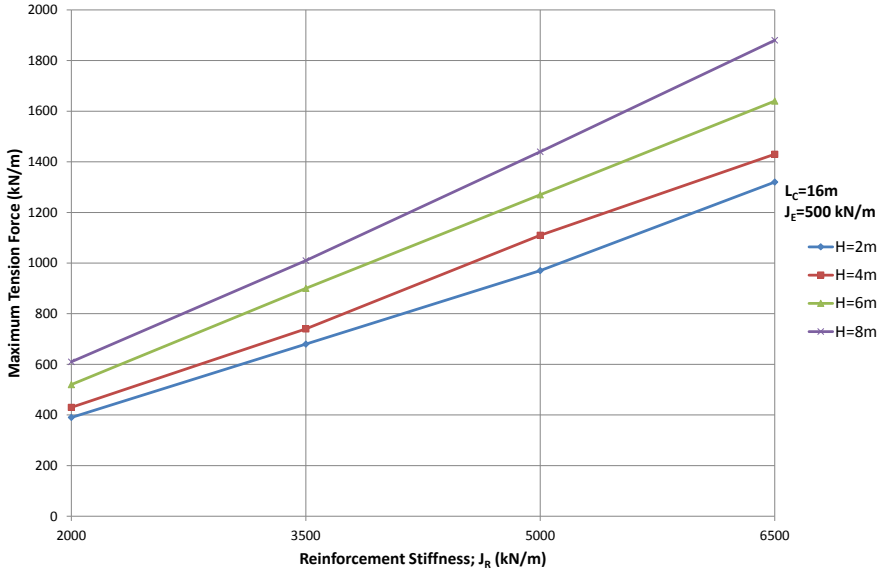

Figure 11. Influence of the reinforcement stiffness on the tension force.

4 CONCLUSIONS

This paper presents a numerical analysis of hypothetical reinforced embankments supported by floating geosynthetic-encased columns. The effects of the basal geogrid reinforcement and the geotextile encasement on the long-term behavior of the modelled geosynthetic reinforced and column-supported embankments are investigated. The following conclusions can be drawn:

1) Surface settlements on both the columns and the soft soil depend on the embankment height.

2) Encasement offers to the columns an increase in the radial stiffness, resulting in a decrease in the columns' bulging. An increase in the encasement stiffness results in a decrease in the lateral column displacement; however, when the stiffness exceeds a certain limiting value, which depends on several aspects, any further decrease in the lateral displacement becomes insignificant. The bulging along the column increases with increasing load, and the bulging zone extends downwards to greater depths during the consolidation. This trend shows that the efficiency of the encasement length is related to the surcharge and the strength properties of the column and the soil.

3) The higher is the stiffness of the basal geogrid reinforcement, the higher is the settlements reduction; however, this relationship is non-linear and similarly like for the encasement stiffness, there is a certain limiting stiffness above which the settlement reduction becomes insignificant.

4) The calculated stress-concentration ratio (SCR) is lower than that recorded in previous studies, which can be attributed to the level of the contribution of the area-replacement ratio, the sand working platform thickness to the column spacing ratio and the fact that the columns are floating and not supported firmly on the base.

5) The maximum computed tensile force in the basal geogrid is consistent with the relatively low computed differential settlement between the columns and the soil. The calculated tensile forces along the geogrid layer decrease as the distance from the center of the embankment increases, i.e., as the surcharge decreases. The maximum tensile force in the geogrid increases in parallel with its tensile stiffness.

Acknowledgments

The authors would like to thank Prof. Ivan Vaníček for his constructive reviews and valuable support throughout the study.

REFERENCES

[1] Hughes, J.M.O., Withers, N.J., Greenwood, D.A. 1975. Field trial of reinforcement effect of a stone column in soil. Geotechnique 25(1), 31–44. doi: 10.1680/geot.1975.25.1.31

[2] Barksdale, R.D., Bachus, R.C. 1983. Design and construction of stone columns. Report FHWA/RD-83/026, National Information Service, Springfield, Virginia.

[3] Borges, J.L., Marques, D.O. 2011. Geosynthetic-reinforced and jet grout column-supported embankments on soft soils: Numerical analysis and parametric study. Computers and Geotechnics 38(7), 883-896. doi: 10.1016/j.compgeo.2011.06.003

[4] Vanicek, I., Vanicek, M. 2008. Earth structures in transport, water and environmental engineering. Springer, Netherlands.

[5] Kempfert, H.G., Stadel, M., Zaeske, D. 1997. Design of geosynthetic-reinforced bearing clayers over piles. Bautechnik 74(12), 818–825.

[6] Raithel, M., Kempfert, H.G. 2000. Calculation models for dam foundations with geotextile-coated sand columns. In Proceedings of International Conference on Geotechnical and Geological Engineering, GeoEng 2000, Melbourne, Australia.

[7] Raithel, M., Kempert, H.G., Kirchiner, A. 2002. Geotextile-encased columns (GEC) for foundation of a dike on very soft soils. Geosynthetics – State of the Art Recent Developments, Delmas, P., Gourc, J. P. & Girard, H., Editors, Balkema, Rotterdam, the Netherlands, pp. 1025–1028.

[8] Raithel, M., Kirchner, A., Schade, C., Leusink, E. 2005. Foundation of construction on very soft soils with geotextile encased columns – state of the art. In Contemporary Issues in Foundation Engineering, Anderson, J. B., Phoon, K. K., Smith, E., Loehr, J. E. ASCE, Reston, VA, USA, Geotechnical Special Publication 131.

[9] Alexiew, D., Brokemper, D., Lothspeich, S. 2005. Geotextile Encased Columns (GEC): load capacity, geotextile selection and pre-design graphs. In Contemporary Issues in Foundation Engineering,

[10] Murugesan, S., Rajagopal, K. 2007. Model tests on geosynthetic encased stone columns. Geosynthetics International 14(6), 346–354. doi: 10.1680/

gein.2007.14.6.346
[11] De Mello, L.G., Mondolf, M., Montez, F., Tsukahara, C.N., Bilfinger, W. 2008. First use of geosynthetic encased sand columns in South America. Proceedings of 1st Pan-American Geosynthetics Conference, Cancu´n Mexico, Industrial Fabrics Association International, Roseville, MN, USA, pp. 1332–1341.
[12] Ayadat, T., Hanna, A.M. 2005. Encapsulated stone columns as a soil improvement technique for collapsible soil. Ground Improvement 9(4), 137–147. doi: 10.1680/grim.2005.9.4.137
[13] Liu, H. L., Ng, C.W.W., Fei, K. 2007. Performance of a geogrid reinforced and pile-supported highway embankment over soft clay: case study. Journal of Geotechnical and Geoenvironmental Engineering 133(12), 1483–1493. doi: 10.1061/(ASCE)1090-0241(2007)133:12(1483)
[14] Murugesan, S., Rajagopal, K. 2010. Studies on the behavior of single and group geosynthetic encased stone columns. Journal of Geotechnical and Geoenvironmental Engineering 136(1), 129-139.
[15] Ali, K., Shahu, J.T., Sharma, K.G. 2012. Model tests on geosynthetic-reinforced stone columns: A comparative study. Geosynthetics International 19(4), 292–305. doi: 10.1680/gein.12.00016
[16] Yoo, C., Lee, D. 2012. Performance of geogrid-encased stone columns in soft ground: full-scale load tests. Geosynthetics International 19(6), 480 –490. doi: 10.1680/gein.12.00033
[17] Hosseinpour, I., Almeida, M.S.S., Riccio, M. 2015. Full-scale load test and finite-element analysis of soft ground improved by geotextile-encased granular columns. Geosynthetics International 22(6), 428-438. doi: 10.1680/jgein.15.00023
[18] Lee, C. J., Bolton, M.D., Al-Tabbaa, A. 2002. Numerical modeling of group effects on the distribution of drag loads in pile foundations. Geotechnique 52(5), 325-335.
[19] Murugesan, S., Rajagopal, K. 2006. Geosynthetic-encased stone columns: Numerical evaluation. Geotextiles and Geomembranes 24(6), 349–358. doi: 10.1016/j.geotexmem.2006.05.001
[20] Yoo, C., Kim, S.B. 2009. Numerical modeling of geosynthetic encased stone column-reinforced ground. Geosynthetic International 16(3), 116–126. https://doi.org/10.1680/gein.2009.16.3.116
[21] Gniel, J., Bouazza, A. 2009. Improvement of soft soils using geogrid encased stone columns. Geotextiles and Geomembranes 27(3), 167–175. doi: 10.1016/j.geotexmem.2008.11.001
[22] Yoo, C. 2010. Performance of geosynthetic-encased stone columns in embankment construction: Numerical investigation. Journal of Geotechnical and Geoenvironmental Engineering 136(8), 129–139.
[23] Khabbazian, M., Kaliakin, V.N., Meehan, C.L. 2011. Performance of quasilinear elastic constitutive models in simulation of geosynthetic encased columns. Computers and Geotechnics 38(8), 998–1007.
[24] Elsawy, M.B.D. 2013. Behavior of soft ground improved by conventional and geogrid-encased stone columns, based on FEM study. Geosynthetics International 20(4), 276–285. doi: 10.1680/gein.13.00017
[25] Almeida, M.S.S., Hosseinpour, I., Riccio, M. 2013. Performance of a geosynthetic-encased column (GEC) in soft ground: Numerical and analytical studies. Geosynthetics International 20(4), 252–262. doi: 10.1680/gein.13.00015
[26] Hosseinpour, I., Riccio, M., Almeida, M.S.S. 2014. Numerical evaluation of a granular column reinforced by geosynthetics using encasement and laminated disks. Geotextiles and Geomembranes 42(4), 363–373. doi: 10.1016/j.geotexmem.2014.06.002
[27] Yoo, C. 2015. Settlement behavior of embankment on geosynthetic-encased stone column installed soft ground - A numerical investigation. Geotextiles and Geomembranes 43, 484-492. doi: 10.1016/j.geotexmem.2015.07.014
[28] Van Eekelen, S.J.M., Bezuijen, A. 2008. Considering the basic starting points of the design of piled embankments in the British Standard BS8006. In: Proceedings of EuroGeo4 p.p. 315, September 2008, Edinburgh, Scotland.
[29] EBGEO 2010. Recommendations for Design and Analysis of Earth Structures using Geosynthetic Reinforcements, German Geotechnical Society (DGGT), Berlin, Germany.
[30] Alexiew, D., Raithel, M., Kuster, V., Detert, O. 2012. 15 years of experience with geotextile encased granular columns as foundation system. ISSMGE-TC 211 Int. Symp. on Ground Improvement IS-GI, ISSMGE TC211 and BBRI, Brussels, Belgium.
[31] Han, J., Gabr, M.A. 2002. Numerical analysis of geosynthetic reinforced and pile-supported earth platforms over soft soil. Journal of Geotechnical and Geoenvironmental Engineering 128(1), 44–53. doi: 10.1061/(ASCE)1090-0241(2002)128:1(44)
[32] Abdullah, C.H., Edil, T.B. 2007. Behavior of geogrid-reinforced load transfer platforms for embankment on rammed aggregate piers. Geosynthetics International 14(3), 141–153. doi: 10.1680/gein.2007.14.3.141
[33] Smith, M., Filz, G. 2007. Axisymmetric numerical

modeling of a unit cell in geosynthetic-reinforced, column-supported embankments. Geosynthetics International 14(1), 13–22. doi: 10.1680/gein.2007.14.1.13

[34] Chen, R.P., Chen, Y.M., Han, J., Xu, Z.Z. 2008. A theoretical solution for pile-supported embankments on soft soils under one-dimensional compression. Canadian Geotechnical Journal 45(5), 611–623. doi: 10.1139/T08-003

[35] Jelušič, P., Žlender, B. 2018. Optimal design of piled embankments with basal reinforcement. Geosynthetics International 25(2), 150–163. doi: 10.1680/jgein.17.00039

[36] Bhasi, A., Rajagopal, K. 2015. Numerical study of basal reinforced embankments supported on floating/end bearing piles considering pile-soil interaction. Geotextiles and Geomembranes 43, 524-536. doi: 10.1016/j.geotexmem.2015.05.003

[37] Khabbazian, M., Meehan, C.L., Kaliakin, V.N. 2015. Column supported embankments with geosynthetic encased columns: Validity of the unit cell concept. Geotechnical Geological Engineering 33, 425–442. doi: 10.1007/s10706-014-9826-8

[38] Jenck, O., Dias, D., Kastner, R. 2009. Three-dimensional numerical modeling of a piled embankment. International Journal of Geomechanics 9(3), 102–112. doi: 10.1061/(ASCE)1532-3641(2009)9:3(102)

[39] Zhang, N., Shen, S.L., Wu, H., Chai, J., Xu, Y., Yin, Z. 2015. Evaluation of effect of basal geotextile reinforcement under embankment loading on soft marine deposits. Geotextiles and Geomembranes 43, 506-514. doi: 10.1016/j.geotexmem.2015.05.005

[40] Satibi, S. 2009. Numerical analysis and design criteria of embankments on floating piles (A PhD thesis submitted to the Universitat of Stuttgart, Stuttgart, Germany).

[41] EBGEO 2010. Recommendations for Design and Analysis of Earth Structures using Geosynthetic Reinforcements, German Geotechnical Society (DGGT), Berlin, Germany. doi: 10.1002/9783433600931

[42] Van Eekelen, S.J.M., Bezuijen, A., Van Tol, A.F. 2011. Analysis and modification of the British Standard BS8006 for the design of piled embankments. Geotextiles and Geomembranes 29, 345-359. doi: 10.1016/j.geotexmem.2011.02.001

[43] Raju, V.R. 1997. The behaviour of very soft soils improved by vibro replacement. Ground Improvement Conference, London.

[44] Brinkgreve, R.B., Vermeer, P.A. 2012. PLAXIS 3D-Finite element code for soil and rocks analysis, Balkema, Rotterdam, The Netherlands.

[45] Kaliakin, V.N., Khabbazian, M., Meehan, C.L. 2012. Modeling the behavior of geosynthetic encased columns: influence of granular soil constitutive model. International Journal of Geomechanics 12(4), 357–369. doi: 10.1061/(ASCE)GM.1943-5622.0000084

[46] Lee, K.L., Seed, H.B. 1967. Drained strength characteristics of sands. J Soil Mech. Found. Div. ASCE, 93, No.6, 117–141.

[47] Ambily, A.P., Gandhi, S.R. 2007. Behavior of stone columns based on experimental and FEM analysis. Journal of Geotechnical and Geoenvironmental Engineering ASCE 133(4), 405–415. doi: 10.1061/(ASCE)1090-0241(2007)133:4(405)

[48] Jelušič, P., Žlender, B. 2018. Optimal design of reinforced pad foundation and strip foundation. International Journal of Geomechanics, 18(9). doi: 10.1061/(asce)gm.1943-5622.0001258

[49] Jelušič, P. & Žlender, B. (2018). Optimal design of pad footing based on MINLP optimization. Soils and Foundations 58(2), 277–289. doi: 10.1016/j.sandf.2018.02.002

[50] Barksdale, R.D., Goughnour, R.R. 1984. Performance of a stone column supported embankment. Proc., Int. Conf. on Case Histories in Geotechnical Engineering, St. Louis, 6–11.

[51] Greenwood, D.A. 1991. Load tests on stone columns. Proc., Deep Foundation Improvements: Design, Construction, and Testing, ASTM, Philadelphia, 148–171.

[52] Rowe, R.K., Soderman, K.L. 1985. An approximate method for estimating the stability of geotextile-reinforced embankments. Canadian Geotechnical Journal 22, 392-398.

[53] Bonapare, R., Christopher, B.R. 1987. Design and construction of reinforced embankments over weak foundations. Transportation. Research Record 1153, 26-39.